International Journal of Fatigue 33 (2011) 842–848

Contents lists available at ScienceDirect

International Journal of Fatigue

journal homepage: www.elsevier.com/locate/ijfatigue

Fatigue crack initiation and growth behavior of Ti–6Al–4V under non-proportional multiaxial loading

H. Nakamura [a,*], M. Takanashi [a], T. Itoh [b], M. Wu [c], Y. Shimizu [c]

[a] Structural Strength Department, Research Laboratory, IHI Corporation, 1, Shin Nakahara-Cho, Isogo-Ku, Yokohama-shi, Kanagawa 235-8501, Japan
[b] Division of Mechanical Engineering, Graduate School of Engineering, University of Fukui, Japan
[c] Graduate School of Engineering, University of Fukui, Japan

ARTICLE INFO

Article history:
Received 31 August 2010
Received in revised form 15 December 2010
Accepted 29 December 2010
Available online 1 January 2011

Keywords:
Multiaxial fatigue
Low cycle fatigue
Titanium alloy
Crack nucleation
Fatigue crack growth

ABSTRACT

This paper deals with multiaxial low cycle fatigue crack behavior of Ti–6Al–4V under non-proportional loading. Strain controlled fatigue tests under proportional loading and non-proportional loading with 90° out-of-phase difference between the axial and shear strains ε and γ were carried out on tubular specimens at room temperature. As a result, Mises strain based fatigue lives under non-proportional loading were approximately 1/10 of those under proportional loading. The specimen surfaces were observed to evaluate life reduction. These results showed that non-proportional loading caused 10 times more cracks than those of proportional loading. Non-proportional loading changes directions of the principal stress and strain axes, and high shear stresses acting on many planes stimulate more slip planes. Consequently, non-proportional loading resulted in many cracks. In addition, the high shear stresses also resulted in larger misorientation under non-proportional loading. The crack initiation life defined as the length $2a$ of 30 μm did not differ significantly between proportional loading and non-proportional loading. However, the fatigue cracks under non-proportional loading propagated faster those under proportional loading. This is because the fatigue cracks under non-proportional loading are subjected to more severe strain field than those under proportional loading, even though the crack size and applied strain are the same. Thus, the significant reduction in fatigue life under non-proportional loading is caused by the accelerated crack growth due to a higher strain intensity factor.

1. Introduction

Ti–6Al–4V has been used for aero engine components because of its excellent specific strength and corrosion resistance. Mechanical structures such as the rotating aero engine components are routinely subjected to thermal stress and body force, and these cyclic loading conditions cause multiaxial low cycle fatigue (LCF). It has been reported that the fatigue lives under the multiaxial LCF non-proportional loading, in which the directions of the principal axes are changed within a cycle, are seriously reduced [1–15]. In general, fatigue life reduction under non-proportional loading is accompanied by an additional strain hardening. Several studies have reported the material dependence between life reduction and additional strain hardening [4,5,7,8,13,15]. Among them, only a few papers deal with the multiaxial fatigue of Ti alloys [16–18], and the fatigue behavior under the non-proportional loading has not been clarified yet.

In this study, strain controlled fatigue tests were conducted on Ti–6Al–4V using proportional loading and non-proportional loading. Observations on microcrack initiation and propagation were carried out by replicating the specimen surface during the fatigue tests. Since electron back-scattering diffraction (EBSD) measurements could identify crystal misorientation which relates to fatigue damage [19], the EBSD measurements were used to evaluate the damage to microstructure under proportional loading and non-proportional loading. The fracture mechanism under non-proportional loading will be discussed in view of additional hardening, microcrack initiation and propagation and crystal misorientation.

2. Materials and experimental procedure

2.1. Material and specimen

Table 1 shows the chemical composition of the Ti–6Al–4V used. The material was forged and subjected to the following heat treatment: 960 °C for 1 h with water-cooling, and 705 °C for 2 h. with air-cooling. The bimodal α and β microstructure in Fig. 1 was obtained after the heat treatment. Table 2 lists the mechanical properties of the material at room temperature. The shape of the specimen for fatigue tests is shown in Fig. 2. The dimensions of

* Corresponding author. Tel.: +81 45 759 2864.
E-mail address: hiroshi_nakamura_2@ihi.co.jp (H. Nakamura).

0142-1123/$ - see front matter © 2011 Elsevier Ltd. All rights reserved.
doi:10.1016/j.ijfatigue.2010.12.013

Table 1
Chemical composition of Ti–6Al–4V (in wt.%).

C	V	Al	N	Fe	O	H	Ti
0.002	4.16	6.30	0.004	0.16	0.20	0.006	Bal.

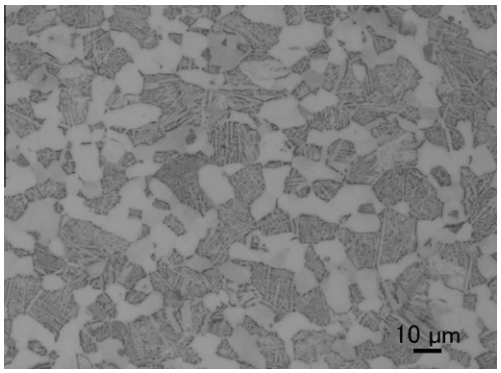

Fig. 1. Microstructure of Ti–6Al–4V.

Table 2
Mechanical properties of Ti–6Al–4V alloy.

Elastic modulus (GPa)	0.2% Proof stress (MPa)	Tensile strength (MPa)
118	943	1017

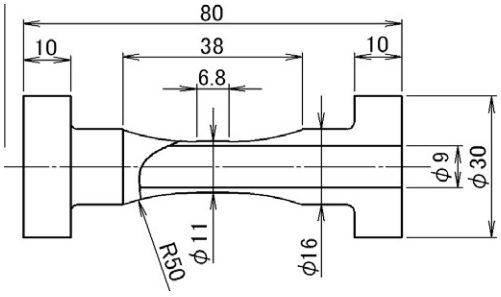

Fig. 2. Geometry and sizes of specimen (in mm).

the specimen were 6.8 mm for the parallel part, 9 mm inner diameter and 11 mm outer diameter in the gage part.

2.2. Fatigue test and multiple step test

Fig. 3 shows strain paths in this study. ε and γ are axial and shear strains, respectively. There are two types of proportional paths. PP is the push–pull path and TP is the torsion path. CP represents 90° out-of-phase loading which is a non-proportional path. The Mises equivalent strain controlled tests at the strain rate of 0.1%/s or 0.5%/s were carried out at room temperature. The strain rate of 0.1%/s was used for short fatigue life. On the other hand, 0.5%/s was used for higher cycle region to reduce testing time. All of the tests were conducted at fully reversed conditions, i.e. strain ratio R of -1. The number of cycles to failure, N_f, was determined as the cycle at which the axial or shear stress amplitude decreased by 25% from its cyclically stable value. The multiple step tests with increasing strain levels were conducted to examine the additional hardening effect due to non-proportional loading. Strain sequence for the test is illustrated in Fig. 4. Stress–strain relationship was obtained after 10 cycles at each strain level. Strain paths for the multiple step tests were PP and CP at the strain rate of 0.1%/s.

2.3. Replicating fatigue crack

Information on microcrack initiation and propagation was obtained by replicating the specimen surface with RepliSet (Struers A/S). Replication was performed for the specimen with Mises strain range $\Delta\varepsilon_{eq} = 1.2\%$ at selected cycles. The replicas were observed with a laser microscope (manufactured by Keyence Corp., VK-9700), and were examined at a magnification of 400 times. Crack initiation was defined as a crack length $2a$ of 30 μm because a crack of 30 μm was identifiable at this magnification. The observed area was 2.5×2.2 mm^2 centered on a critical crack leading to fatigue failure.

2.4. Surface preparation and conditions for EBSD measurements

After the fatigue test, specimens of $\Delta\varepsilon_{eq} = 1.2\%$ and 1.7% were used for the EBSD measurements. The samples were observed at their uncracked portions. The surface of the sample was polished using 1 μm aluminum oxide followed by colloidal silica (Struers

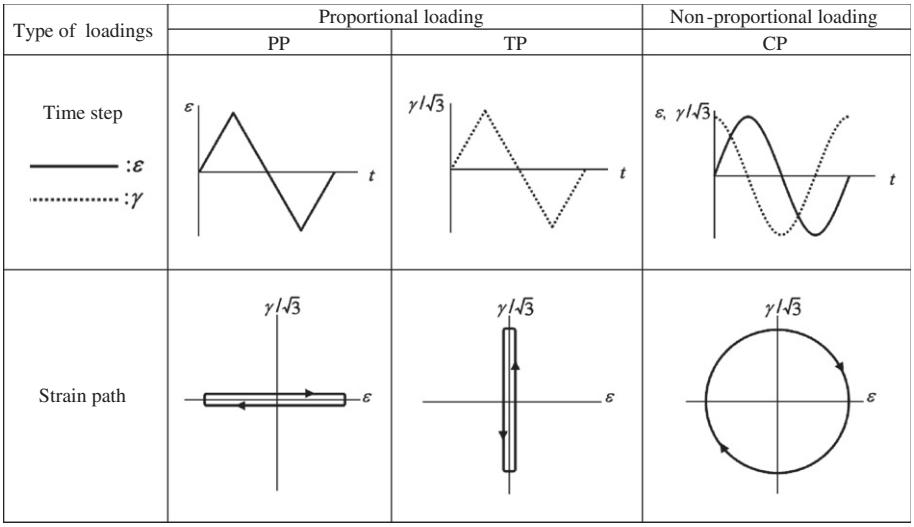

Fig. 3. Strain paths employed.